Supporting Information:

Reassessment of the Four-Point Approach to the Electron Transfer Marcus-Hush Theory

Omar López-Estrada[†],[*] Humberto G. Laguna[†], Cihuapilli Barrueta-Flores[†], and Carlos Amador-Bedolla[†*]

[†] *Departamento de Física y Química Teórica, Facultad de Química, Universidad Nacional Autónoma de México, Cd. Universitaria, Av. Universidad 3000, CP 04510, Ciudad de México, México*

E-mail: omar.lopez.e@gmail.com; carlos.amador@unam.mx

Transition state energy for $k_1 \neq k_2$

Let us start with properly generalized Equations 1 for the parabolas in Figure 2 of the manuscript,

$$\begin{aligned} G_1(x) &= G_1^0 + k_1(x - x_1)^2, \\ G_2(x) &= G_2^0 + k_2(x - x_2)^2 \end{aligned}$$

and find the intersection by solving,

$$(k_2 - k_1)x^2 - 2(k_2x_2 - k_1x_1)x + \left(G_2^0 - G_1^0 + k_2x_2^2 - k_1x_1^2\right) = 0,$$

then we get the analytical solution

$$x_\pm = \frac{k_2x_2 - k_1x_1 \pm \sqrt{\Delta G^0\ (k_1 - k_2) + k_1\ k_2\ (x_2 - x_1)^2}}{k_2 - k_1}$$

and rewriten it as,

$$x_\pm = \frac{k_2x_2 - k_1x_1 \pm \sqrt{1 + \frac{\Delta G^0\ (k_1 - k_2)}{k_1\ k_2\ (x_2 - x_1)^2}}}{k_2 - k_1}$$

it is apparent that the first term of the Taylor expansion (valid for $k_1 \approx k_2$) are

$$x_+ = \frac{\Delta G^0 + k_2x_2^2 - k_1x_1^2}{2(k_2x_2 - k_1x_1)},$$

and

$$x_- = \frac{2(k_1x_1 - k_2x_2)}{k_1 - k_2},$$

From the analytical solution we found the transition state energy

$$\Delta G^{\dagger} = \frac{k_1\left[k_2\ (x_2 - x_1) \pm \sqrt{k_1\ k_2\ (x_2 - x_1)^2\left(1 + \frac{\Delta G^0\ (k_1 - k_2)}{k_1\ k_2\ (x_2 - x_1)^2}\right)}\ \right]^2}{(k_2 - k_1)^2}.$$

whose first order term of their Taylor expansion, $\Delta G^{\dagger}_{+}$ (for $k_1 \approx k_2$) is presented in Equation 4 of the manuscript.

In comparison with the symmetric Marcus-Hush theory, the existence of two distinct curvatures ($k_1 \neq k_2$) introduces two intersection points between the parabolas (Figure S1). The left intersection point has coordinates $(x_a, G(x_a))$, and the physically pointless energy barrier can be estimated by $\Delta G_{x_a} = G(x_a) - G^0_1$. At this point an interesting question appears, can Marcus-Hush formula (Equation 2 of the manuscript) distinguish the physical situation from the non-physical one? Employing the quadratic equations the coordinates of the minimum in each parabola (x_1, G^0_1, x_2, G^0_2) and their corresponding curvatures (k_1 and k_2 respectively) can be calculated as summarized in Table 2 of the manuscript. From the knowledge of the analytical parameters the energy barrier for the parabolas in Figure S1 can be obtained. Results are summarized in Table S1 where the last two columns show the data obtained by means of the Taylor series approximation (Equation 4 of the manuscript).

From the data in Table S1, the consistency between the Taylor expansion solution (Equation 4 of the manuscript that yields Marcus-Hush formula when $k_1 = k_2$) and the analytical one can be checked. The result is remarkable because the x_+ value obtained by means of the Taylor expansion is far from both the unphysical and physical solutions. Hence the approximated value ($\Delta G^{\dagger}_{+}$) is far from the analytical result ($\Delta G^{\dagger}$). It should also be mentioned that the first order Taylor expanded x_- solution is even worse, as expected from the divergence of the corresponding expression ($x_- = 4.487$ and $\Delta G^{\dagger}_{-} = 0.4455$).

We emphasizes that the approximate solution presented in equation 4 of the manuscript is accurate only in the vicinity of $k_1 \approx k_2$, and any deviation from that situation leads to wrong values, as can be concluded from the results shown in Table S1. For this system

the ratio between curvatures is $k_1/k_2 \approx 2.02$, and the value obtained by the approximate solution is two orders of magnitude larger than the analytical result.

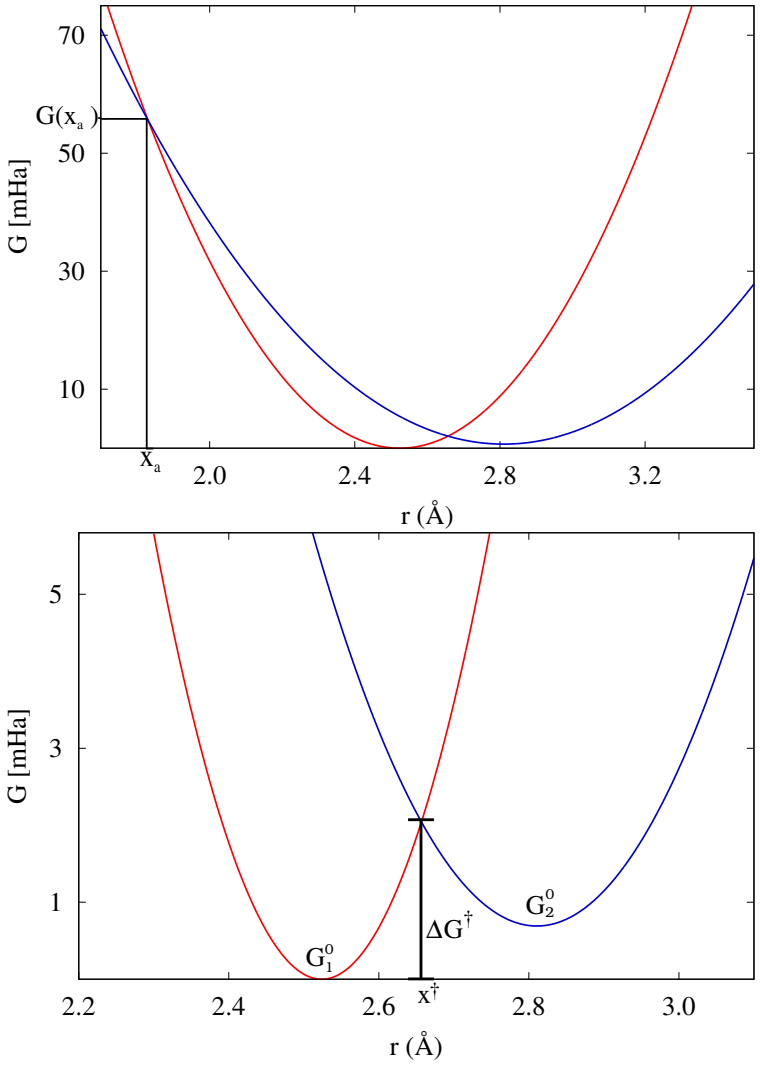

Figure S1: Top: Free Gibbs energy for the ${}^3\Sigma_g^-$ (blue) and ${}^3\Pi_u$ (red) electronic states employing the analytical quadratic equation. Bottom: The local minima ($G_1^0(x_1)$ and $G_2^0(x_2)$) are expanded and $\Delta G^\dagger$ is shown.

Table S1: Reaction coordinates (in Å) for the non-physical intersection point x_a, the physical $x^\dagger$, and the obtained by the Taylor expansion $x_+^\dagger$. Their respective energy barriers ΔG (in Hartrees) are indicated.

x_a	ΔG_{x_a}	$x^\dagger$	$\Delta G^\dagger$	$x_+^\dagger$	$\Delta G_+^\dagger$
1.830	0.0556	2.657	$2.044(10^{-3})$	1.084	0.2397

Energetic properties of the studied molecules

Table S2: Total energy (E in Hartrees) and Gibbs free energy (G in Hartrees) in their respectively ID geometries (Figure 5) for the neutral optimized structures (Opt) and the anion single point (SP) computations at the geometries obtained after been optimized at the ωB97XD/cc-pVTZ theory level.

	Neutral Opt		Anion SP	
ID	E	G	E	G
A1	-845.7633	-845.6953	-845.8277	-845.7623
A2	-601.1618	-601.1036	-601.2490	-601.1978
A3	-1485.1249	-1485.1010	-1485.2496	-1485.2286
A4	-778.4139	-778.3950	-778.4940	-778.4790
A5	-678.5386	-678.4506	-678.6660	-678.5800
A6	-575.1447	-574.9469	-575.0768	-574.8819
A7	-1188.9379	-1188.8063	-1189.0262	-1188.8933
A8	-872.5784	-872.4342	-872.6345	-872.4900
A9	-1026.2288	-1026.0373	-1026.3012	-1026.1095
A10	-1192.7191	-1192.5380	-1192.7853	-1192.6054
A11	-1749.8174	-1749.5756	-1749.8982	-1749.6627
A12	-1605.3791	-1605.0296	-1605.3791	-1605.0296
D1	-468.1427	-467.9120	-468.0698	-467.8511
D2	-389.5189	-389.3451	-389.4462	-389.2728
D3	-366.2155	-366.0731	-366.1453	-366.0132
D4	-385.8775	-385.7588	-385.8547	-385.7431
D5	-614.9391	-614.7628	-614.9019	-614.7369
D6	-578.8210	-578.6345	-578.8293	-578.6467
D7	-655.0628	-654.8635	-655.0664	-654.8729
D8	-556.7700	-556.6001	-556.7413	-556.5785
D9	-693.1548	-692.9508	-693.1272	-692.9258
D10	-1036.7472	-1036.4555	-1036.7259	-1036.4418

Table S3: Total energy (E in Hartrees) and Gibbs free energy (G in Hartrees) in their respectively ID geometries (Figure 5) for the anion optimized structures (Opt) and the neutral single point (SP) computations at the geometries obtained after been optimized at the ωB97XD/cc-pVTZ theory level.

	Anion Opt		Neutral SP	
ID	E	G	E	G
A1	-845.8379	-845.7733	-845.7524	-845.6819
A2	-601.2542	-601.1990	-601.1567	-601.0976
A3	-1485.2593	-1485.2364	-1485.1152	-1485.0900
A4	-778.5084	-778.4917	-778.3997	-778.3803
A5	-678.6735	-678.5872	-678.5314	-678.4426
A6	-575.0810	-574.8873	-575.1404	-574.9422
A7	-1189.0356	-1188.9063	-1188.9283	-1188.7946
A8	-872.6447	-872.5024	-872.5683	-872.4216
A9	-1026.3095	-1026.1182	-1026.2206	-1026.0259
A10	-1192.7954	-1192.6195	-1192.7088	-1192.5251
A11	-1749.9078	-1749.6698	-1749.8075	-1749.5640
A12	-1605.4327	-1605.0906	-1605.3719	-1605.0209
D1	-468.0799	-467.8589	-468.1307	-467.8994
D2	-389.4581	-389.2918	-389.5085	-389.3313
D3	-366.1567	-366.0237	-366.2028	-366.0618
D4	-385.8606	-385.7492	-385.8717	-385.7541
D5	-614.9094	-614.7424	-614.9310	-614.7563
D6	-578.8342	-578.6532	-578.8161	-578.6295
D7	-655.0718	-654.8785	-655.0575	-654.8584
D8	-556.7474	-556.5854	-556.7637	-556.5941
D9	-693.1296	-692.9309	-693.1520	-692.9481
D10	-1036.7309	-1036.4469	-1036.7340	-1036.4422

Table S4: Differences between data calculated with $\bar{\lambda}_1$ and $\bar{\lambda}_3$ plotted in Figure 7 of the paper. $\Delta\Delta G^\dagger = \Delta G^\dagger(\bar{\lambda}_3) - \Delta G^\dagger(\bar{\lambda}_1)$ in eV.

D-A pair	$\Delta\Delta G^\dagger$	D-A pair	$\Delta\Delta G^\dagger$	D-A pair	$\Delta\Delta G^\dagger$
A2-D9	1.676	A3-D6	0.073	A11-D3	0.029
A2-D4	0.542	A11-D8	0.073	A4-D10	0.028
A2-D8	0.341	A12-D10	0.068	A9-D10	0.027
A3-D9	0.295	A3-D10	0.066	A9-D8	0.024
A2-D6	0.246	A7-D1	0.062	A5-D6	0.023
A2-D2	0.243	A6-D10	0.061	A3-D3	0.023
A11-D9	0.235	A3-D7	0.057	A8-D1	0.022
A2-D7	0.228	A9-D2	0.053	A1-D10	0.021
A5-D10	0.213	A2-D10	0.052	A5-D8	0.019
A2-D5	0.192	A10-D10	0.050	A12-D5	0.019
A5-D9	0.142	A11-D6	0.047	A11-D10	0.019
A3-D2	0.130	A1-D9	0.046	A4-D4	0.018
A3-D4	0.127	A4-D9	0.044	A1-D4	0.018
A11-D2	0.102	A5-D4	0.042	A8-D2	0.015
A11-D4	0.101	A11-D7	0.042	A9-D6	0.014
A2-D3	0.096	A10-D1	0.039	A7-D2	0.014
A9-D9	0.089	A4-D2	0.037	A12-D3	0.014
A7-D10	0.089	A11-D5	0.037	A4-D8	0.012
A5-D1	0.087	A1-D2	0.036	A1-D8	0.012
A3-D8	0.085	A9-D4	0.035	A9-D7	0.011
A5-D2	0.080	A3-D5	0.031		
A12-D1	0.076	A8-D10	0.030		

Sample Gaussian input files for A1 molecule

Table S5: Gaussian input for computation of the ground state energetic properties of neutral A1 molecule.

```
%chk=str.chk
%mem=60Gb
%nproc=16
# Opt=(CalcFC,MaxCycles=900) Freq wB97XD/cc-pVTZ scf=xqc

Title

0 1
C       0.29007864  -0.73747037   0.00068200
C       1.68523864  -0.73747037   0.00068200
C       2.38277664   0.47028063   0.00068200
C       1.68512264   1.67878963  -0.00051700
C       0.29029764   1.67871163  -0.00099600
C      -0.40730336   0.47050563   0.00000000
H      -0.25968036  -1.68978737   0.00113200
H       3.48245664   0.47036063   0.00131600
H      -0.25982436   2.63099263  -0.00194900
N       2.42060380   2.95156905  -0.00059587
N      -1.87730332   0.47075027  -0.00024063
N       2.41981133  -2.01077311   0.00243987
O       3.20284022  -2.08087188   1.11219296
O       3.20050133  -2.08528723  -1.10867253
O       2.09369446   3.66398426  -1.11198908
O       2.09095115   3.66570710   1.10887967
O      -2.33092464  -0.16933771   1.11066669
O      -2.33056141  -0.17123053  -1.11020359
```

Table S6: Gaussian input for computation of the single point energetic properties of the anionic A1 but in the coordinates of the ground state neutral A1.

```
%chk=str.chk
%mem=60Gb
%nproc=16
# Freq  wB97XD/cc-pVTZ  scf=xqc  geom=check

Title

-1 2
```

Calculation of the activation energy of D1-A1 pair

First we remember that the reaction we consider is

$$A1 + D1^- \longrightarrow A1^- + D1$$

We follow Figure 1 of the manuscript. Computation of the minimun of the left parabola, $G_1(x_1)$, requires the ground state of the neutral A1 species (-845.6953 Ha from Table S2 above) and the ground state of the anionic D1 species (-467.8589 Ha from Table S3 above). Suming these two Free Gibbs energies we get $G_1(x_1) = G_1^0 = -1313.5542$ Ha.

Conversely, computation of the minimun of the right parabola, $G_2(x_2)$, requires the ground state of the anionic A1 species (-845.7733 Ha from Table S3 above) and the ground state of the neutral D1 species (-467.9120 Ha from Table S2 above). Suming these two Free Gibbs energies we get $G_2(x_2) = G_2^0 = -1313.6853$ Ha.

Then $\Delta G^0 = -0.1311$ Ha.

Now computation of $G_2(x_1)$, requires a single point calculation of the anionic A1 species but in the coordinates of the neutral ground state of A1 (-845.7623 Ha from Table S2 above) and a single point calculation of the neutral D1 species but in the coordinates of the the anionic ground state of D1 (-467.8994 Ha from Table S3 above). Suming these two Free Gibbs energies we get $G_2(x_1) = -1313.6617$ Ha.

Conversely, computation of $G_1(x_2)$, requires a single point calculation of the neutral A1 species but in the coordinates of the anionic ground state of A1 (-845.6819 Ha from Table S3 above) and a single point calculation of the anionic D1 species but in the coordinates of the the neutral ground state of D1 (-467.8511 Ha from Table S2 above). Suming these two Free Gibbs energies we get $G_1(x_2) = -1313.5330$ Ha.

Now, computation of the reorganization energies requires proper equation similar to

equation 3 of the manuscript. First we proceed to compute λ_1 through

$$G_2(x_1) - G_1(x_1) = \lambda_1 + \Delta G^0,$$

$$\lambda_1 = -1313.6617 + 1313.5542 + 0.1311 = 0.0236 \;\; Ha$$

and to compute λ_2 we use

$$G_1(x_2) - G_2(x_2) = \lambda_2 - \Delta G^0,$$

$$\lambda_2 = -1313.5330 + 1313.6853 - 0.1311 = 0.0212 \;\; Ha.$$

Reorganization energies in eV are,

$$\lambda_1 = 0.642 \;\; eV,$$

$$\lambda_2 = 0.577 \;\; eV.$$

Now we proceed to compute the different averages according to equations 8−11 of the manuscript, and substitute them in equation 2 of the manuscript in order to compute the activation energies. Results are presented in the following table.

Table S7: Activation energies $\Delta G^{\dagger}$ (in eV) computed with the different reorganization energies for the D1-A1 pair.

λ	$\Delta G^{\dagger}$
λ_1	3.879
λ_2	3.337
$\bar{\lambda}_1$	3.593
$\bar{\lambda}_2$	3.608
$\bar{\lambda}_3$	3.600
$\bar{\lambda}_4$	3.600

Figures

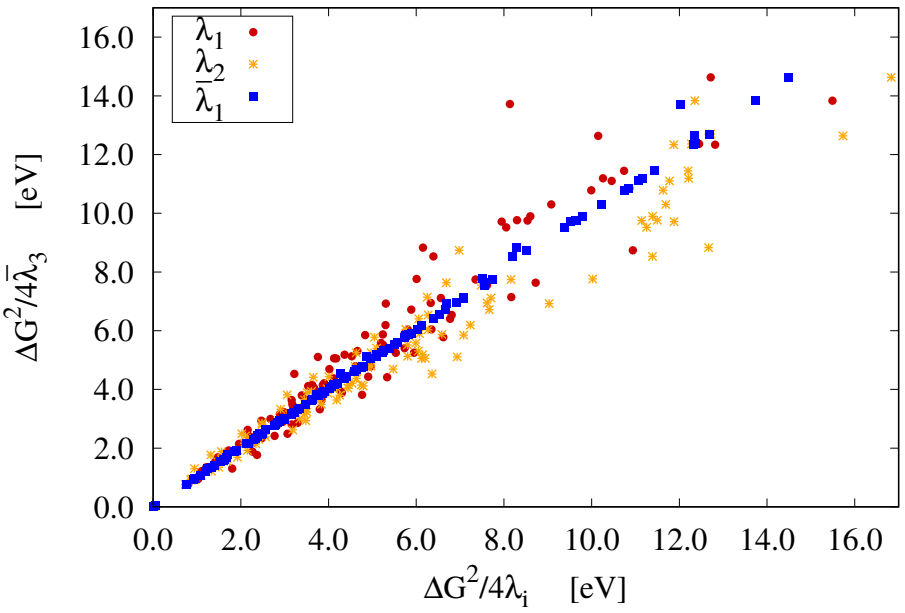

Figure S2: Comparison of $\frac{\Delta G^2}{4\lambda}$ calculated with $\bar{\lambda}_1$, λ_1 or λ_2 and those calculated with $\bar{\lambda}_3$.

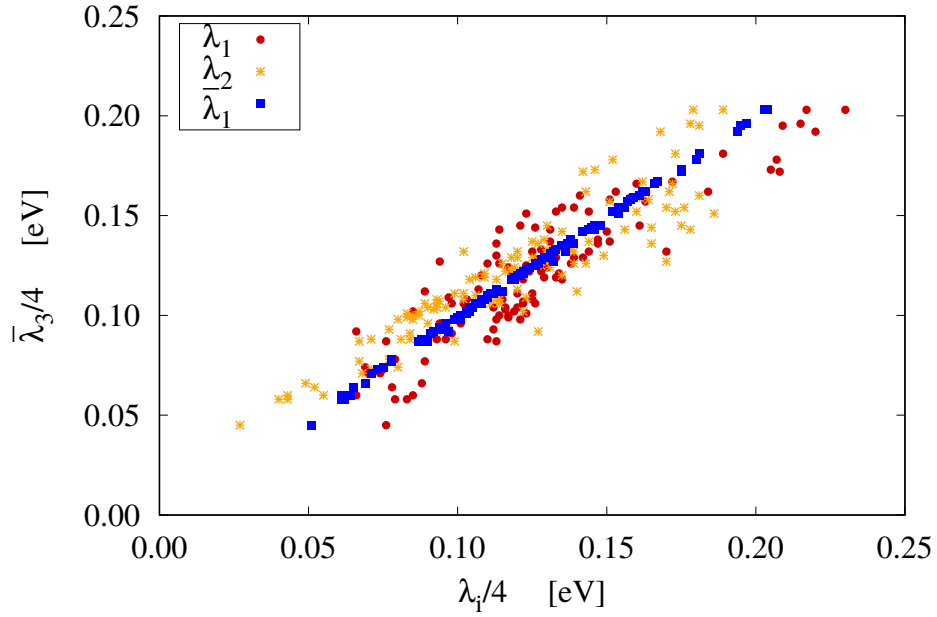

Figure S3: Comparison of $\frac{\lambda}{4}$ calculated with $\bar{\lambda}_1$, λ_1 or λ_2 and those calculated with $\bar{\lambda}_3$.

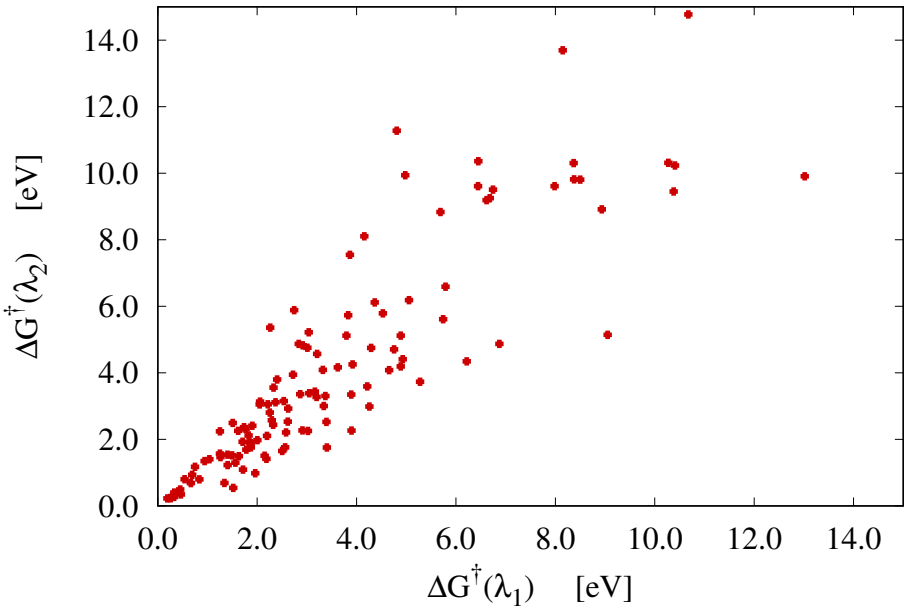

Figure S4: Comparison of $\Delta G^{\dagger}$ calculated with λ_1 and λ_2. Equation of the linear fit is $f(x) = 1.130x + 0.207$, with $R^2 = 0.682$.

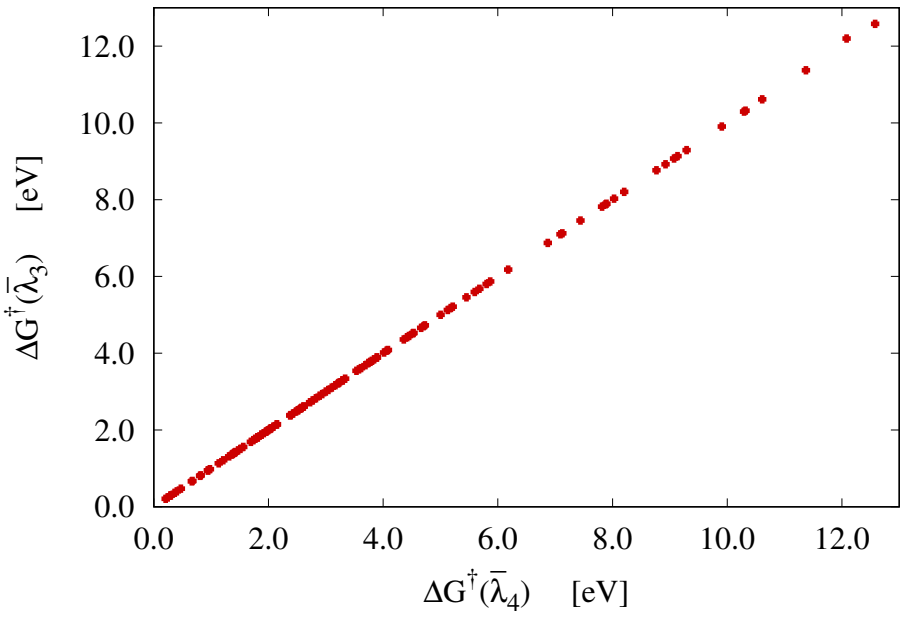

Figure S5: Comparison of $\Delta G^{\dagger}$ calculated with $\bar{\lambda}_3$ and $\bar{\lambda}_4$. Equation of the linear fit is $f(x) = 1.001x - 0.003$, with $R^2 = 0.999987$.

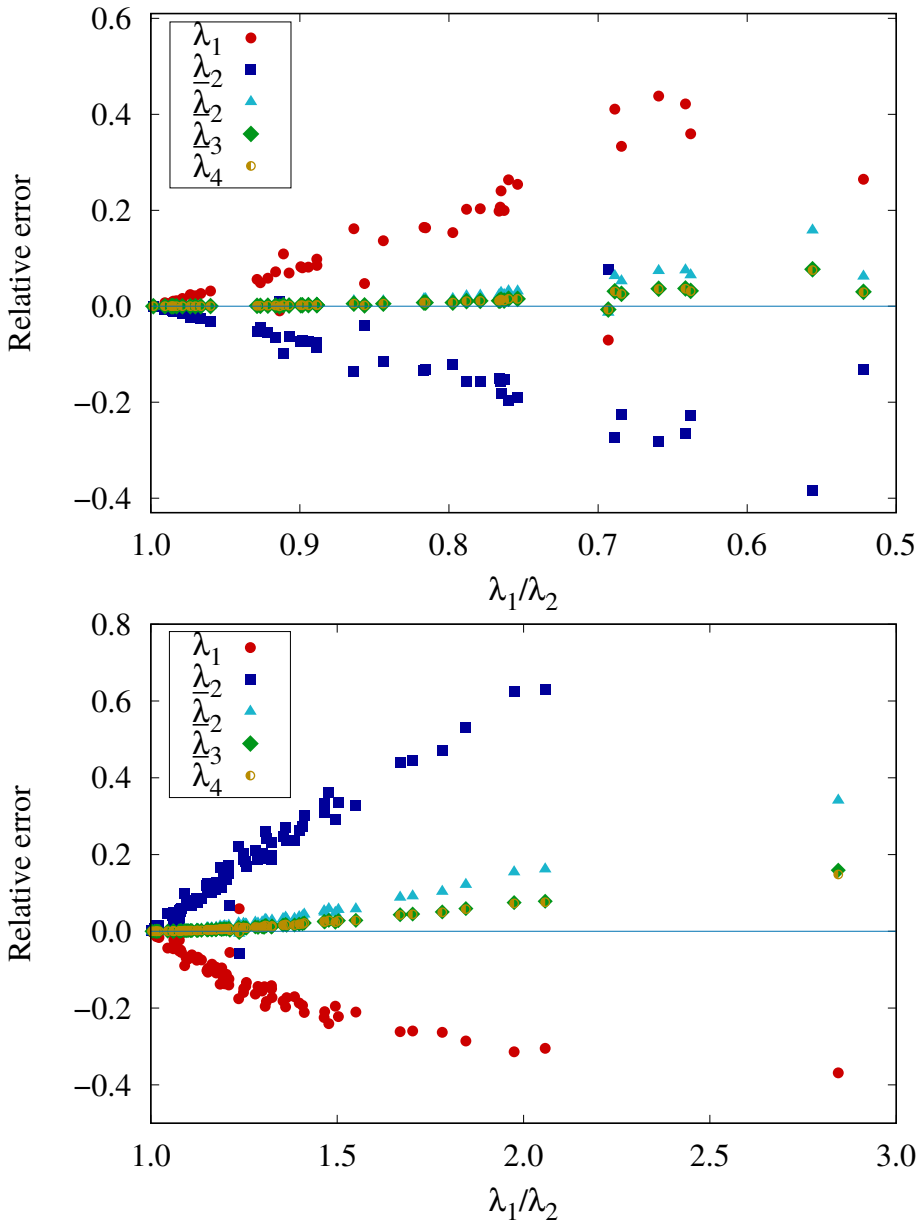

Figure S6: Variation of the relative error in the calculation of the transition state energy ($\Delta G^{\dagger}$) from Marcus formula with λ_1, λ_2, $\bar{\lambda}_2$, $\bar{\lambda}_3$ and $\bar{\lambda}_4$ with respect to the reference $\bar{\lambda}_1$, as a function of the reorganization energies ratio, λ_1/λ_2. Values for all the 120 DA pairs are shown. Top: $\lambda_1 < \lambda_2$ case. Bottom: $\lambda_1 > \lambda_2$ case.

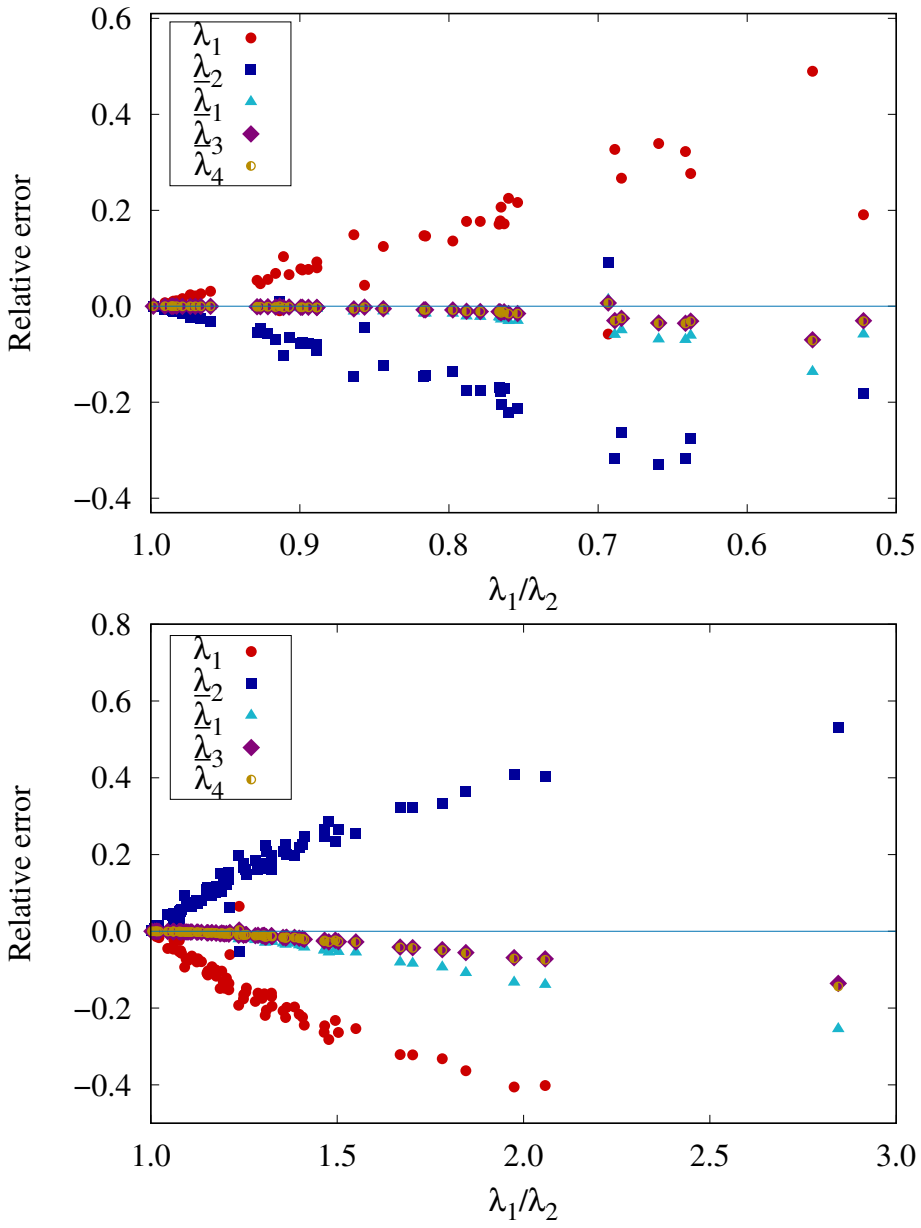

Figure S7: Variation of the relative error in the calculation of the transition state energy ($\Delta G^{\dagger}$) from Marcus formula with λ_1, λ_2, $\bar{\lambda}_1$, $\bar{\lambda}_3$ and $\bar{\lambda}_4$ with respect to the reference $\bar{\lambda}_2$, as a function of the reorganization energies ratio, λ_1/λ_2. Values for all the 120 DA pairs are shown. Top: $\lambda_1 < \lambda_2$ case. Bottom: $\lambda_1 > \lambda_2$ case.

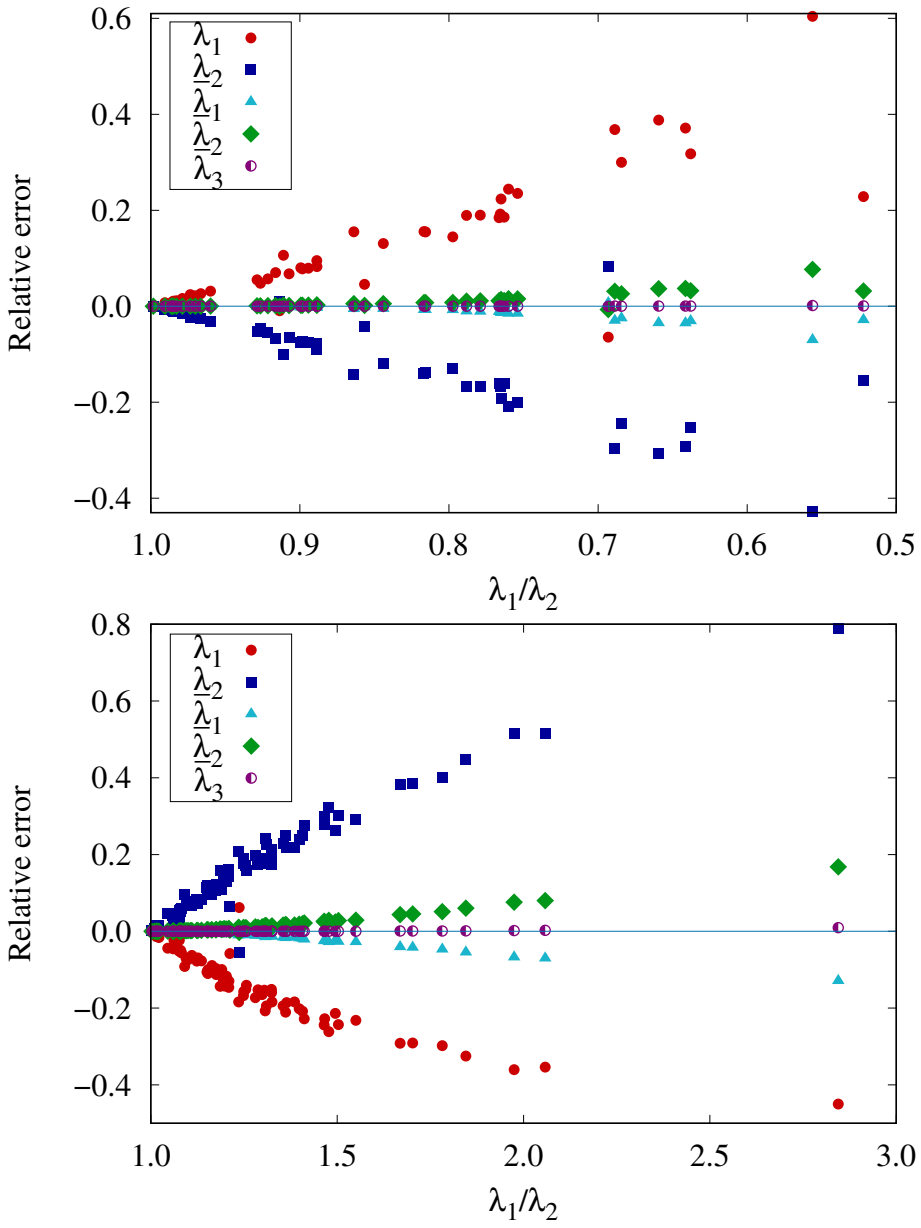

Figure S8: Variation of the relative error in the calculation of the transition state energy ($\Delta G^{\dagger}$) from Marcus formula with λ_1, λ_2, $\bar{\lambda}_1$, $\bar{\lambda}_2$ and $\bar{\lambda}_3$ with respect to the reference $\bar{\lambda}_4$, as a function of the reorganization energies ratio, λ_1/λ_2. Values for all the 120 DA pairs are shown. Top: $\lambda_1 < \lambda_2$ case. Bottom: $\lambda_1 > \lambda_2$ case.

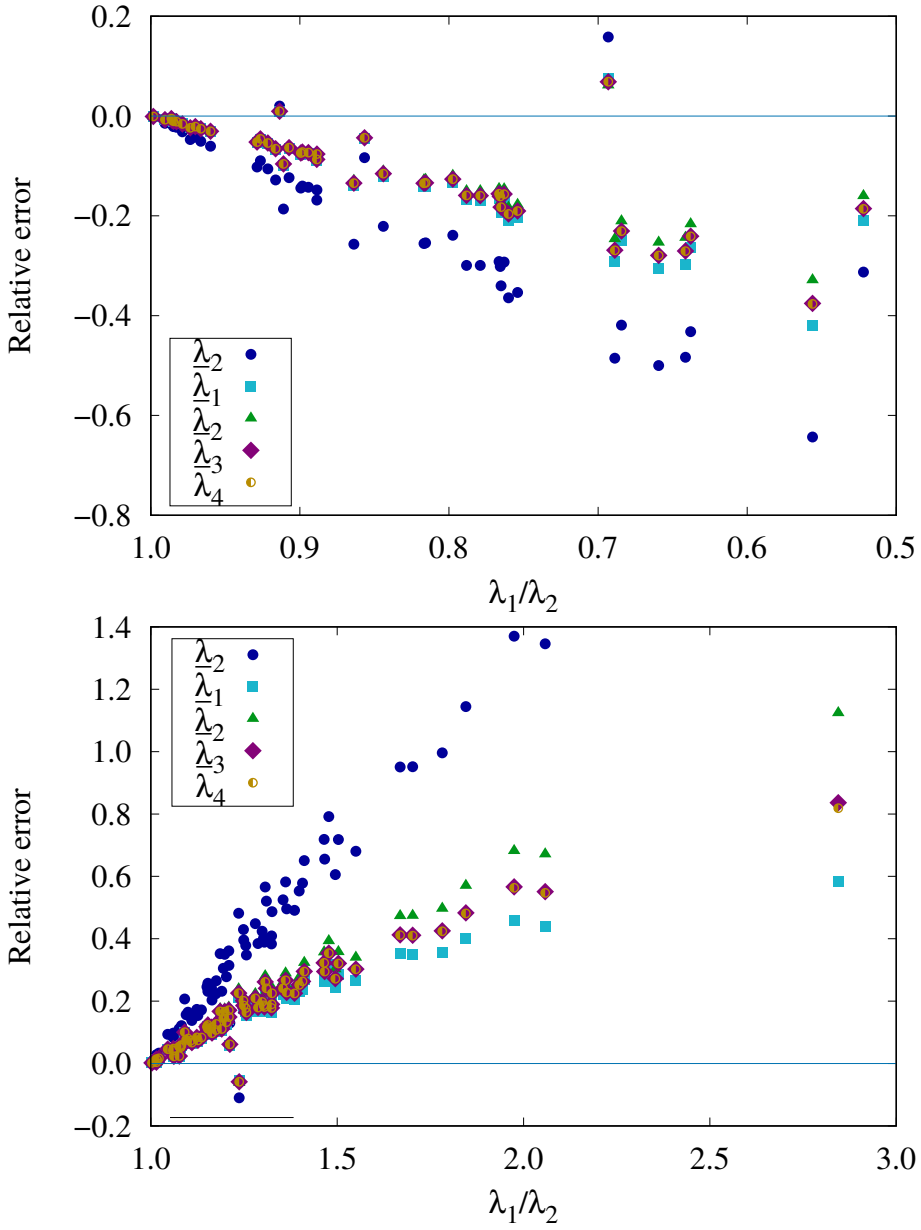

Figure S9: Variation of the relative error in the calculation of the transition state energy ($\Delta G^{\dagger}$) from Marcus formula with λ_2, $\bar{\lambda}_1$, $\bar{\lambda}_2$, $\bar{\lambda}_3$ and $\bar{\lambda}_4$ with respect to the reference λ_1, as a function of the reorganization energies ratio, λ_1/λ_2. Values for all the 120 DA pairs are shown. Top: $\lambda_1 < \lambda_2$ case. Bottom: $\lambda_1 > \lambda_2$ case.

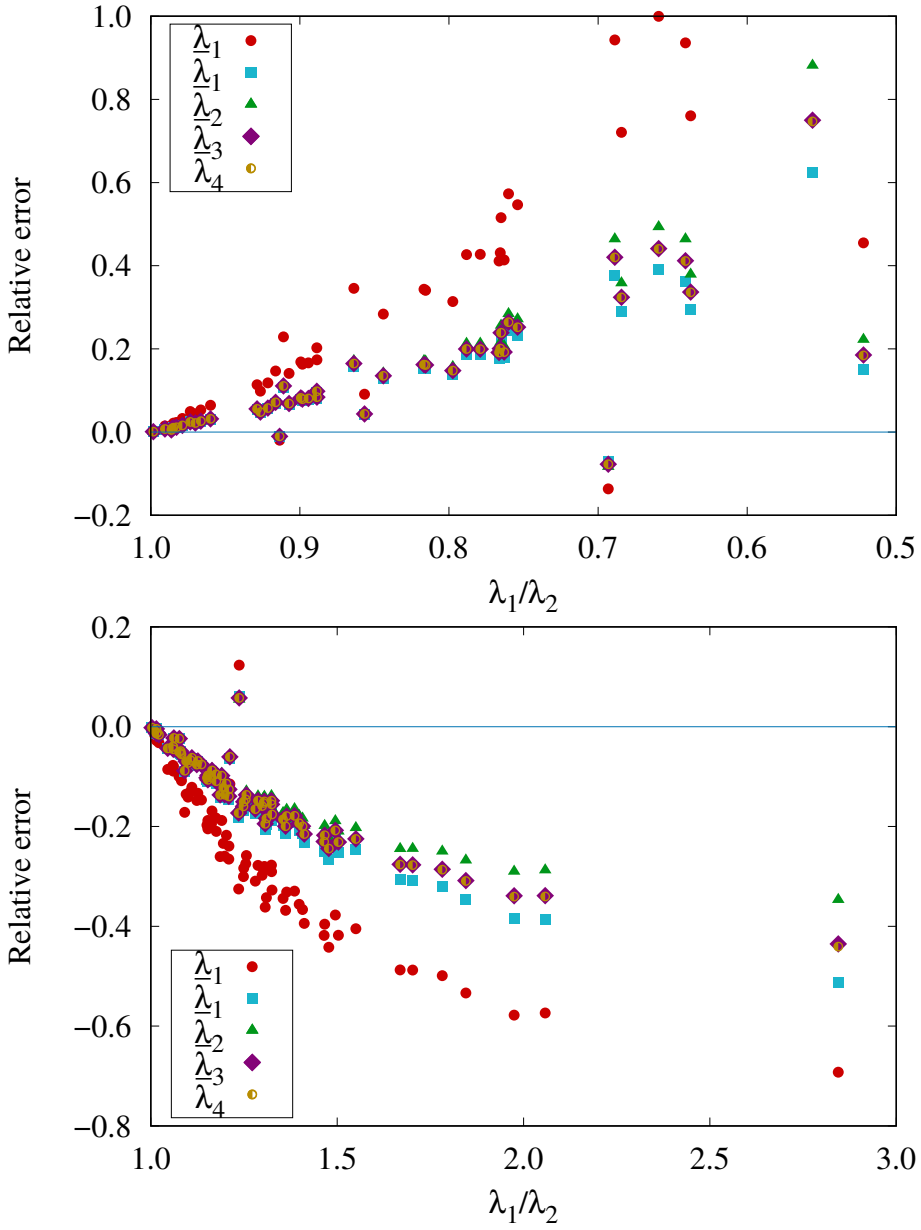

Figure S10: Variation of the relative error in the calculation of the transition state energy ($\Delta G^{\dagger}$) from Marcus formula with λ_1, $\bar{\lambda}_1$, $\bar{\lambda}_2$, $\bar{\lambda}_3$ and $\bar{\lambda}_4$ with respect to the reference λ_2, as a function of the reorganization energies ratio, λ_1/λ_2. Values for all the 120 DA pairs are shown. Top: $\lambda_1 < \lambda_2$ case. Bottom: $\lambda_1 > \lambda_2$ case.